Electrogeneration and Characterization of Poly(methylene Blue) Thin Films on Stainless Steel Electrodes. Effect of the pH.

José Juan García-Jareño *, Jerónimo Agrisuelas, Zoe Vargas *, Francisco Vicente

Posted Date: 4 July 2024

doi: 10.20944/preprints202407.0460.v1

Keywords: Methylene Blue; Stainless Steel 316; Polymerization; pH dependence; kinetics mechanism; Digital Video Electrochemistry (DVEC).

Article

Electrogeneration and Characterization of Poly(methylene blue) Thin Films on Stainless Steel Electrodes. Effect of the pH

José Juan García-Jareño [1,*], Jerónimo Agrisuelas [1], Zoe Vargas [1] and Francisco Vicente [1]

Departament Química-Física, Universitat de València, Dr. Moliner 50, 46100 Burjassot (Spain)
* Correspondence: jose.j.garcia@uv.es; Tel.: (+34 963543992)

Abstract: Methylene blue has been electropolymerized on the surface of a stainless steel 316. The addition of sodium oxalate and working at a pH near 11 has allowed to obtain steel electrodes coated with electroactive polymer. This polymer shows electrochromic properties similar to those of the monomer, but also appears electroactivity at more positive potentials which is associated to the active centers in the bridges between monomeric units. The study by means of digital video electrochemistry has allowed on the one hand, to quantify the color changes on the entire surface of the stainless steel simultaneously and by means of the mean color intensities to separate the contribution to the overall polymer response of the active centers of the phenothiazine ring and of the inter-monomer bonds. A reduction mechanism for the polymer compatible with the pH variation of the observed electrochemical behavior is proposed.

Keywords: methylene blue; stainless steel 316; polymerization; pH dependence; kinetics mechanism; digital video electrochemistry (DVEC)

1. Introduction

Conductive polymers (CPs) have emerged as an exciting class of materials that are attracting significant interest for their conductive properties that have made it possible to replace metals in some applications or semiconductors of an inorganic nature[1]. This was thanks to the discovery of polyacetylene (PA) by Hideki Shirakawa, Alan MacDiarmid and Alan Heeger[2], from which numerous other conductive polymers with similar properties were synthesized, such as polyphenylene (PP)[3], polyphenylenevinylene (PPV)[4], polypyrrole (PPy)[5,6], (PTh) [7] and polyaniline (PANI) [8,9]. Nowadays, a large number of different monomers are known to form conductive polymers[4,10].

The huge challenge lies in achieving precise control of the electrical or electrochemical properties of the CPs. Despite their advantages, like their chemical diversity, low density, flexibility, corrosion resistance and ability to easily control their shape and morphology, as well as their adjustable conductivity compared to other inorganic equivalents, they still have inherent limitations in terms of solubility, conductivity and long-term stability. Consequently, research has been driven towards the creation of CP-based complexes and hybrids with innovative structures, leading to the development of materials with high mechanical stability, flexibility and conductivity. This has significantly expanded their applications as key components in light-emitting diodes, transistors, electronic actuators and other devices[1].

CP synthesis usually involves the oxidation of the monomer by oxidizing agents or the application of electric potential or current through electrodes[11]. Thanks to the system of alternating single (σ) and double (π) bonds present in CPs, these π conjugated systems could acquire electrically conductive properties by losing electrons through oxidation or by receiving electrons through reduction. Therefore, the oxidation of CPs generates a p-type doped state and reduction generates an n-type doped state[12]. This makes that conductivity of CPs can also be controlled by these redox reactions[11]. As in non-conductive polymers, the general physical properties of CPs depend on their

 doi:10.20944/preprints202407.0460.v1

size, length and molecular weight[11] that in the case of conductive polymers can be modulated by the electrogeneration experimental conditions.

Among these types of conductive polymers, poly(phenothiazines) and poly(phenazines)[13,14] are worth mentioning. These monomers are characterized by a central aromatic group and two more or less methylated amino groups at the two ends. These monomers have been used as dyes since they show intense absorption bands at wavelengths in the visible. It is known that after polymerization, this polymer retains a color similar to that of the monomer, which suggests that the chromophore group is not highly affected after polymerization. For example, many poly(phenothiazines) have a characteristic blue color (poly(Azure A), poly(methylene blue), etc.). In the case of poly(phenazine) such as poly(Neutral Red) the characteristic red color of this polymer as contrasted with the blues of the phenothiazines confirms the idea that the chromophore group is the central aromatic group of the monomer. However, after polymerization it has been reported new absorption bands at wavelengths in the near IR that are associated with the bonds between monomeric units[15]. Consequently, the use of spectroelectrochemical techniques may be the best option to characterize this type of materials and the mechanisms by which the oxidation and reduction processes take place.

One of these monomers despite being known for years may gain attention in the coming years due to different properties that make it very interesting in different applications. Methylene blue (MB) (Figure 1) was first reported by the German chemist Heinrisch Caro in 1876, a few years later in 1886 Dr. Paul Ehrlich proved that MB stains living neurons and also plasmodium, the parasite that causes malaria. It was later found to have properties that inhibited the transmission of malaria[16]. More recent research suggests that this pigment may also be useful in other treatments for neurodegenerative diseases or cancer. Even in the recent COVID-19 pandemic, it has been studied how it inhibits the interaction between the SARS-CoV-2 spike protein and angiotensin-converting enzyme 2 (ACE2), which is key in virus infection[17].

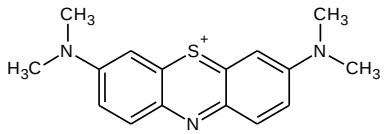

Figure 1. Chemical Structure of Methylene Blue.

Another interesting feature of MB is its characteristic blue color. The phenothiazine ring absorbs radiation at wavelengths between 630 and 680 nm, giving the characteristic blue color to this type of compound. This absorption can lead to the formation of reactive oxygen species (ROS), such as singlet oxygen $^1O_2$ It is precisely these ROS that can destroy cancer cells and control their growth. This means that this material can also be used in photodynamic therapies to control the proliferation of cancer cells or other diseases[18–20]. One of the key points in these electrochemical pollutant removal processes is precisely energy consumption. The possibility of generating ROS by absorption of electromagnetic radiation can lead to a significant reduction in the consumption of electrical energy for normal operation. All this makes the optical properties of these materials of great interest for the design of these applications.

It is also important to keep in mind that for these materials to be used in some of these applications it is necessary for the MB to be fixed to some kind of support. In the case of medicinal applications to aid localized application and in the case of electrochemical applications, a good electronic conductor is necessary for it to be used as an electrode. The possibility of applying electromagnetic radiation to produce ROS would suggest that electrodes that do not absorb electromagnetic radiation but reflect it could significantly improve the efficiency. If we add to all this the fact that the substrate has good mechanical properties, it is not particularly expensive and it is easy to recover, stainless steel 316 (SS316) is a perfect candidate as a substrate to fix the MB.

Another problem with the use of MB is that it must be firmly attached to the substrate and not solubilized in aqueous media where it is to be employed. Simple adsorption on the substrate surface may not be sufficient. At this point a good strategy is to electropolymerize the MB on SS316, which has the advantage of improving its retention on SS316. Once polymerized, it will be necessary to

 doi:10.20944/preprints202407.0460.v1

check that the polymer retains the same optical and electrochemical properties of the monomer that make it interesting for applications that require the production of controlled ROS or for anion-cation insertion.

However, this material (the steel) also has some drawbacks to generate polymers on its surface. On SS316 electrodes at the potentials where the radical cation is generated, ROS and Fenton-like processes are also favored due to the presence of iron cations[21,22]. It is well known that mineralization of MB can be achieved by Fenton-like processes in different experimental conditions[23–25] and if that happens, it should be impossible to get a good quality polymer. This difficulty must be overcome before the polymer can be obtained on the surface of the SS316.

As mentioned above, the optical-spectroscopic properties of these materials are very important to accurately describe their oxidation or reduction mechanisms, since these involve color changes. Spectroelectrochemistry makes it possible to simultaneously follow absorbance variations at single or multiple wavelengths and current changes during an electrochemical process[5,26,27]. However, it requires the use of dark working conditions, and absorbance is measured only in a small region of the electrode surface. In an opaque electrode, as in our case, reflectance would have to be measured and the signal intensity would be quite dependent on the angle of incidence-reflection. If the electrode surface did not reflect electromagnetic radiation, it would not be possible to follow color changes in these materials by spectrophotometric measurements. In recent years, a spectroelectrochemistry modality has been developed based on the acquisition of videos of the electrode surface during the experiment. The video frames are separated and treated as independent images. A region of the image is selected to follow its temporal evolution. For this purpose, the mean intensity of each color channel (Red, Green and Blue) and the standard deviation of each color intensity in the analyzed region are obtained. This technique is known as digital video electrochemistry (DVEC) and has been used to monitor the quality of metallic electrodeposits or conductive polymers, to obtain kinetic constants of electrochemical processes or to measure the rate and the extend of electrochemical processes in different parts of the electrode in a simulated manner[28–32].

The main objectives of this research are essentially two. On the one hand, it is to optimize the electrodeposition process on SS316. As is well known, SS316 can oxidize under certain conditions and the surface of the metal will change its conductive properties, as there will be layers of metal oxides that can become insulating and therefore prevent its use as an electrode. The generation of the polymer requires the application of sufficiently positive potentials where the oxidation of the metal can occur. The first objective is to avoid this oxidation and other possible parallel reactions and ensure that only the oxidation of the monomer takes place so that the polymerization process can begin.

Secondly, once the polymer has been electrogenerated, it is necessary to verify that it retains the redox and chromatic properties of the monomer, in addition to verifying that the polymer is firmly fixed to the steel surface so that it can be used in different applications. For this purpose, its electrochromic response at different pH will be investigated to study in depth the mechanism by which the redox processes of the polymer take place.

2. Results

2.1. Electropolymerization on Stainles Steel 316

The first stage in this study is the generation of poly(methylene blue) on the SS316 surface. As mentioned in the introduction section, the generation of the polymer requires the prior formation of cation radicals at sufficiently positive potentials. In the case of steels, at these potentials and depending on the medium, oxidation of the metal can also take place, and at the end of the electrogeneration there is no fixed polymer on the electrode surface.

As an example, Figure 2 shows that if the deposition is carried out under similar conditions to those performed on more stable electrodes such as gold, upon reaching sufficiently positive potentials, oxidation and pitting of the SS316 surface occurs, and although the surface apparently has a blue color, when this electrode is studied by cyclic voltammetry in an aqueous medium, the blue color of the surface disappears and the solution is intensely blue colored. This leads to the suspicion

 doi:10.20944/preprints202407.0460.v1

that the blue color on the surface is just adsorbed monomer, weakly adhered to the surface of the SS316.

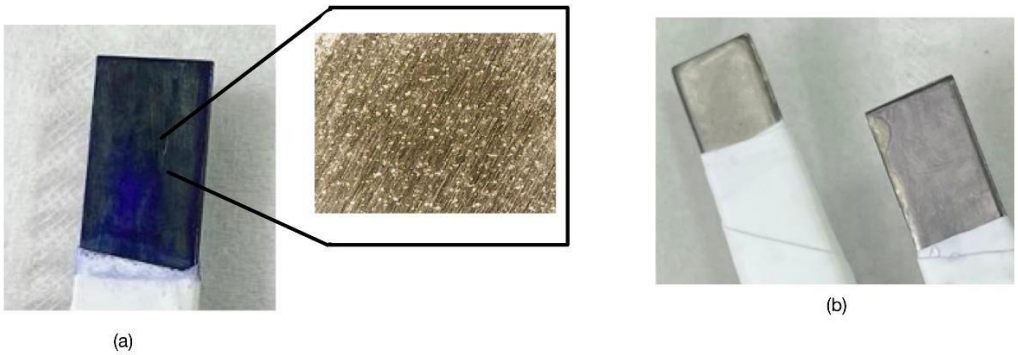

Figure 2. (a) Methylene Blue Deposit in acidic medium with pitting formation, showing a very intense blue. (b) Electrode after characterization in 0.5M KCl that has lost color (right), compared to an unused SS316 electrode (left).

As discussed in the Introduction section, one of the compounds that is relatively easy to remove from water by Fenton-type advanced oxidation processes is methylene blue. Moreover, during the process of generating the cation radical, it is evident in Figure 2 how pitting corrosion of the steel has occurred, which has released cations of different metals into the solution that are known to favor this type of advanced oxidation processes.

To try to overcome these problems, a different electropolymerization strategy is being tested. On the one hand, in recent studies for polyaniline and poly(neutral red) is has been proved that the presence of oxalate anions can stabilize the monomer, and then polymerization takes place[33,34] on SS316 electrodes. On the other hand, to try to avoid that the metallic cations can pass into the solution, it will be tested to increase the pH. In addition, the chlorides that favor the formation of pitting are removed from the medium.

Figure 3 shows the appearance of the polymer-coated SS316 electrode and how after the characterization study, the electrode appears a less intense blue color although it still maintains a good electrochromic response.

Figure 3. (a) Freshly electrogenerated PMB on SS316 in basic medium, free of Cl^- anions and with $C_2O_4^{2-}$, (b) PMB on SS316 after characterization in 0.5 M KNO_3 solution. RGB coordinates of each blue electrode were marked.

After several trial-and-error tests, optimum generation conditions were achieved on the freshly polished electrode surface by performing up to 100 voltammetric cycles in the potential range from -0.4 V to 1.0 V against the reference electrode Ag|AgCl at a sweep speed of 20 mV s^{-1}. The monomer solution is brought to pH near 11 and in the presence of oxalate anions, (see Materials and Methods Section).

 doi:10.20944/preprints202407.0460.v1

Figure 4 shows how the current evolves during the polymer growth experiment. In the region marked as (e) (potentials 0.8-1.0 V) is where the generation of the monomer cation radical and the polymer growth occurs. At more negative potentials, during the first few cycles only a system of peaks marked (a) and (b) is observed for the anodic and cathodic peaks, respectively, which are associated with oxidation-reduction processes of the phenothiazine ring. As the number of cycles increases a new system of voltammetric peaks appears (peaks (c) and (d)) which were not observed during the first cycles. This system is associated with the electroactivity of the new bridges or bonds between monomeric units[13,15,30].

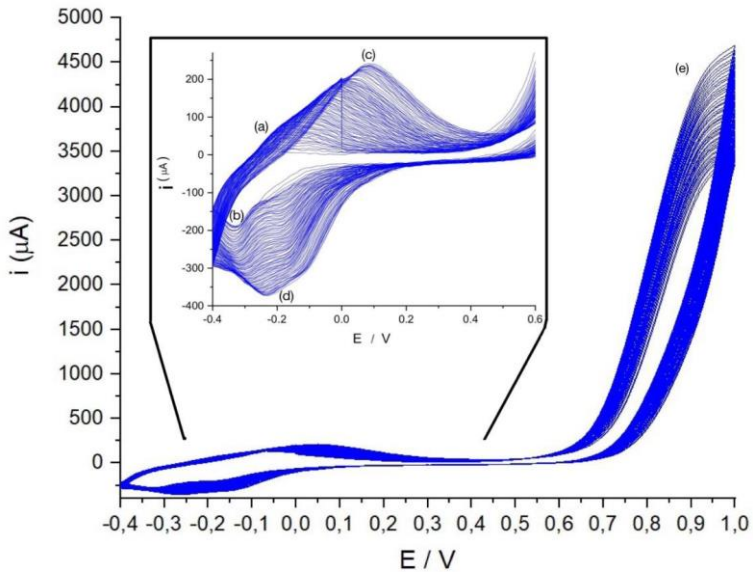

Figure 4. Polymerization of the MB by cyclic voltammetry at potentials ranged from -0.4V to 1.0V, scan rate 20 mV s^{-1}.In this Figure: (a) Anodic peak of MB at -0.22V. (b) Cathodic peak of MB at -0.33V. (c) Anodic peak of PMB at 0.08V. (d) Cathodic peak of PMB -0.23V (e) potentials where the radical cation is formed and the polymerizations takes place.

According to Figure 4 on the one hand, the electroactivity of the phenothiazine ring is maintained in the polymer since the peak system (a)-(b) grows with polymerization and a new peak system appears that can be associated with the bonds between monomers ((c)-(d)) and which also grows with the number of cycles.

2.2. Spatiotemporal Digital Video Electrochemistry Analysis

The digital videoelectrochemistry technique allows simultaneous and quantitative color changes to be obtained over the entire surface of the metal, provided that the solution is transparent. In the case of our SS316 coated with PMB and studied in a 0.5 M KNO_3 solution by cyclic voltammetry, the surface changes to a lighter blue color when the polymer is reduced. Figure 5 shows a 3D map of color intensity increment ($\Delta I_R, \Delta I_G$) or color intensity against the distance to the top of the electrode and the elapsed time during the voltammogram. One first observation is that color changes take place simultaneously, regardless of the distance from the top of the electrode. In other systems, if there is a resistive electrode color change and electrochemical processes take place at different times on the electrode surface[35–37]. In spite of this homogeneity in time it is not the same if we look at the distance from the top of the electrode. Color intensity increment (ΔI_C) proves more evident near the top of the electrode, while color intensity (I_C) changes proved larger at the bottom of the electrode. This discrepancy is explained by the fact that color increment is directly related to the number of active sites that have changed its oxidation state, while the color intensity change is explained because there are fewer active sites at the bottom.

 doi:10.20944/preprints202407.0460.v1

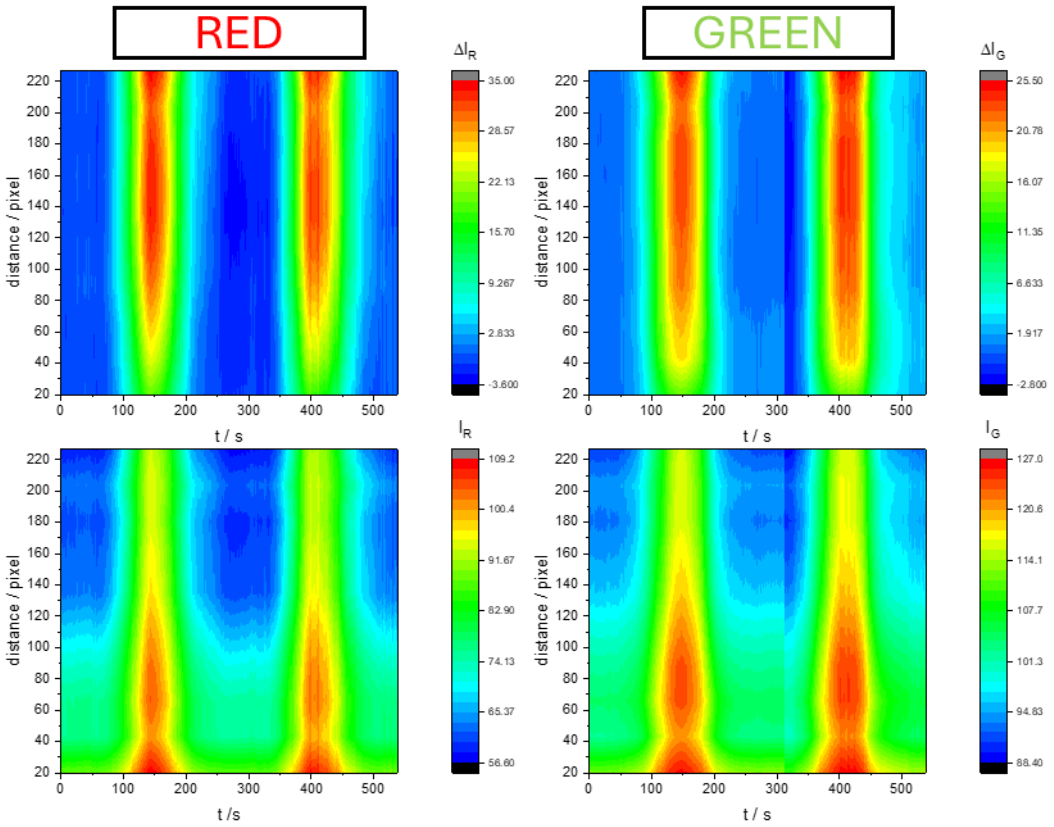

Figure 5. D maps of color evolution during voltammograms of PMB on SS316 electrodes in 0.5 M KNO_3 pH=3.12 solution Scan rate was 10 mV s^{-1}.

In any case, the color changes do not occur as intensely across the whole electrode, possibly because more PMB has been deposited on top. If we want to correlate the color changes with the current during the voltammogram we have to simultaneously analyze the entire electrode surface since the measured current is a global current of the entire electrode surface. For this purpose, the best option is to obtain an average of the color intensity at each pixel for each of the three color coordinates (R,G,B). Note that this spatiotemporal analysis is not possible with a spectrophotometer that only takes the absorbance measurement at a localized region on the electrode surface.

2.3. Identification of Electroactive Sites in the Polymer. Voltammetric Peaks Deconvolution

Once a relatively stable polymer has been obtained on the steel electrode, it is time to characterize its electrochemical behavior. To achieve this, we will use Digital Video Electrochemistry (DVEC) that allows simultaneously recording the current signal during the electrochemical experiment and the video of the color changes that take place on the electrode surface [28,31,32,37,38]. DVEC was not possible for the electrogeneration experiment since the solution was a dark blue color and the electrode surface was masked by the solution. However, for the characterization study all solutions were transparent and it is relatively easy to capture images of the surface of the PMB-coated SS316 electrode.

The use of spectroelectrochemistry in this study aims to separate the different contributions to the electrochemical response in this type of materials[13,15,30]. As commented above, polymerization generates new active centers in the material when compared to the monomer in solution. Fundamentally, the new bridges between monomer units can exhibit electroactivity and also electrochromism[13,15].

First, a voltammogram with its associated color changes is presented in order to be able to assign each color change to different electroactive processes (Figure 6) .

Preprints.org (www.preprints.org) | NOT PEER-REVIEWED | Posted: 4 July 2024 doi:10.20944/preprints202407.0460.v1

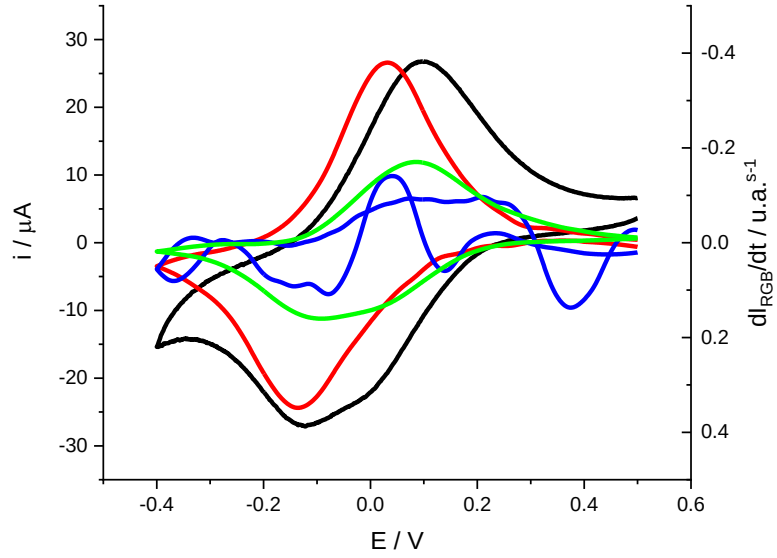

Figure 6. Voltammogram of a PMB polymer generated on SS316 (black line). Experimental conditions: 0.5 M KNO_3 solution, pH= 3.12, scan rate = 0.002 V s^{-1}. Color changes are expressed as mean color intensity derivative for the Red (red line) and Green (green line) and Blue (blue line) components.

Looking at the shape of the cathodic peak current (black line) it proves clear that this not correspond to the shape of a voltametric peak for adsorbed substances accordingly with the Laviron equation[39]. In some cases the shape of the peaks is distorted by non-ideal effects such as resistance or interactions between active centers[35,36,40]. At other times, the peak simply does not correspond to a single electrochemical process and the measured current is the overlapping of different electrochemical processes. [13,30,36]. In the latter case, coupled techniques such as quartz microbalance or spectroscopy can allow separation of the signal associated with different processes.

Figure 6 also includes color changes expressed as the derivative of color intensity versus time. A recent publication has shown that for voltammetric processes with associated color changes, the current i_c is directly related to the derivative of color intensity versus time$\left(\frac{dI_C}{dt}\right)$[32,41].

$$i_C = -\frac{nF}{k_C}\left(\frac{dI_C}{dt}\right) \quad (1)$$

in this expression n is the number of electrons involved in the reaction, F is the Faraday constant and k_C (a.u. mol-1) is a measure of the electrochromic efficiency for each channel and for each process.

The first observation is that both the red and green intensity derivatives show peaks similar to the voltametric peaks, although separated in potential. The peak associated with green appears at more positive potentials while that associated with red appears at more negative potentials. The intensity derivative of blue shows a variation with ups and downs which could indicate that it is associated with some intermediate species that appear and disappear during the redox process[13,30].

If we focus on the red and green components, the separation of peak potentials suggests that they may be associated with different processes. As mentioned above, the use of coupled techniques can allow complex signals to be deconvoluted into their individual components. In this case and according to equation (1) it is possible to estimate the contribution to the overall current associated with each color intensity derivative. For this it is necessary to know the electrochromic efficiency of each color component, or in other words the value of k_C for each color. As this is not possible a priori, we use a least-squares fitting procedure to fit the sum of the contributions to the experimental current according to equation (2)

$$i = \frac{nF}{k_R}\left(\frac{dI_R}{dt}\right) + \frac{nF}{k_G}\left(\frac{dI_G}{dt}\right) \quad (2)$$

 doi:10.20944/preprints202407.0460.v1

This fitting was done for data in the potential range corresponding to the cathodic peak. Electrochromic efficiencies obtained from the fitting are for red and for green $\frac{k_R}{n} = 3.4\,x\,10^9\ (a.u.mol^{-1})$ and $\frac{k_G}{n} = 0.83\,x10^9\ a.u.mol^{-1}$. These are relatively high electrochromic efficiencies, particularly for red and similar to values obtained for poly(o-toluidine)[42]. Figure 7 shows the deconvolution of the electrochemical current response during the voltammogram as the sum of two processes, one associated with the green color change and the other with the red color change.

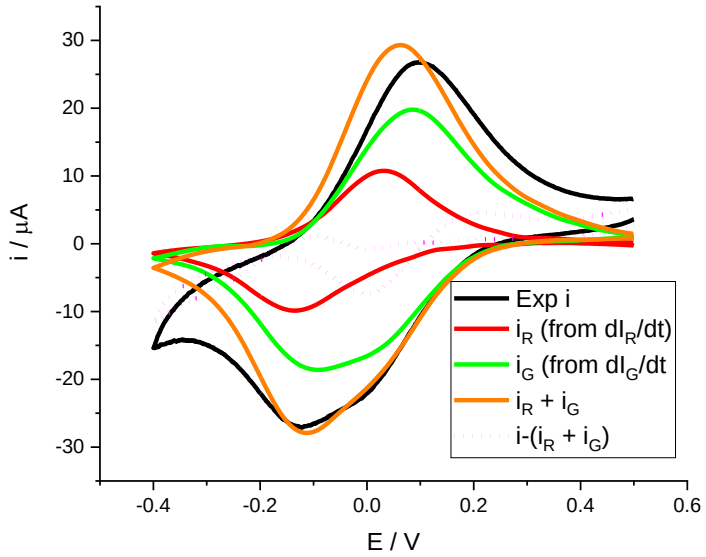

Figure 7. Deconvolution of a voltammogram of a PMB polymer generated on SS316. Experimental conditions: 0.5 M KNO3 solution, pH= 3.12, scan rate = 0.002 V s^{-1}. Black line corresponds to the experimental measured current during the experiment, the red line and the green line represent the current associated to the dI_R/dt and dI_G/dt curves of Figure 6. Dots line represent the difference between experimental current and the contributions of red and green processes.

It is also interesting to note that although the red color change is much more evident, the current associated with this process is much lower than that associated with green. Another interesting fact shown by both the Figure 6 as Figure 7 is that the color intensity derivatives have baseline=0. It is especially observed at more negative potentials, where the current starts to decrease due to the hydrogen evolution reaction (HER). This is why the difference between the experimental current and the sum of the two contributions is especially distinct in this region of the voltammogram. In addition, during the anodic peak, it is observed that the parameters obtained for the cathodic peak do not reproduce the oxidation peak well. The line marking the difference shows discrepancies. This leads us to think that the mechanisms by which reduction takes place are not necessarily the same as for oxidation.

A typical way to characterize an electrochromic device is the contrast (ΔI_C), the difference between maximum and minimum color intensity, equation (3).

$$\Delta I_C = I_{C,max} - I_{C,min} \tag{3}$$

and for a scan rate of 2 mV s^{-1} we obtain a contrast of 51 units for the red component and 27 units for the green component. Assuming that all the active centers have been reduced, that means a surface concentration for the Red active centers 0.015 $\mu mol\ cm^{-2}$ and 0.042 $\mu mol\ cm^{-2}$ for the green active centers. In Figure 4 it is shown that the system of peaks associated with the phenothiazine ring proves smaller than the system of peaks associated with the new bridges between the monomers units. It is compatible with these surface concentrations. The Green color processes could be identified with electrochemical activity of the new bridges and the Red color processes with the phenothiazine ring activity. Note that a pure Blue color surface means a Red color intensity 0, and then if the polymer

Preprints.org (www.preprints.org) | NOT PEER-REVIEWED | Posted: 4 July 2024 doi:10.20944/preprints202407.0460.v1

blanches during reduction, the I_R component should increase. It is not so visible for the I_B since, both the reduced and the oxidized forms are blue. Looking again at Figure 8 one can see that contrast for the Red component proves more dependent on the scan rate. This fact can be interpreted as the phenothiazine ring electroactivity proves slower than the bridges electroactivity of this monomer.

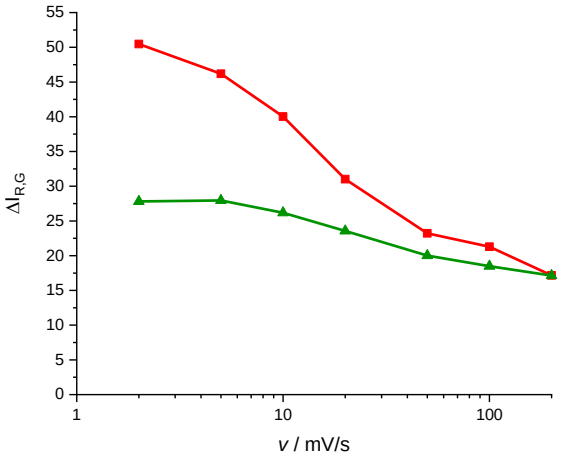

Figure 8. Representation of the contrast of red and green color intensities ΔI_C (equation (3)) versus scan rate (mV s^{-1}) during the CV of the PMB process in a 0.5 M KNO_3 solution, pH = 3.12. Red lines correspond to the red color contrast and green line to the green color contrast.

2.4. Scan Rate Study of Voltammetric Peaks

We present the study of the dependence of the voltammetric curves on the scan rate. The most commonly used model to describe the voltammetric curves of conductive polymers deposited on electrodes is the classical model in which electroactive substances (oxidized and reduced) are adsorbed on the electrode surface. In this case, symmetrical voltammetric peaks are obtained, ideally there is no separation between the cathodic and anodic peak and the height of the peaks is similar. When the scan rate is changed, the peak intensity increases linearly with the scan rate accordingly to the Laviron model[39]. Since it seems possible to identify each color derivative with a different electrochemical (electroactive center) process we study the dependence of electrochemical current peak (i_p), and the maximum of color derivatives for the Red and Green components, $\left(\frac{dI_R}{dt}\right)_p$ and $\left(\frac{dI_G}{dt}\right)_p$, respectively (Figure 9).

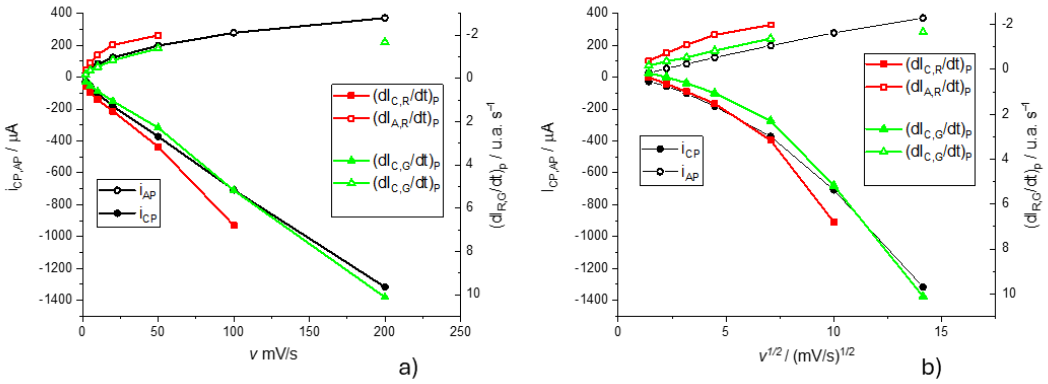

Figure 9. Anodic and cathodic peak currents and and the maximum of color derivatives for the Red and Green components against the scan rate (a) and against the square root of the scan rate. In this context, i is the electrical current and dIc/dt the color intensity derivative for the color C.

 doi:10.20944/preprints202407.0460.v1

Subindex C and A make reference to the cathodic and anodic processes, respectively. All experiments were carried out in a 0.5 M KNO_3 pH=3.12 at different scan rates. Open symbols are for anodic peaks and filled symbols for cathodic peaks.

It is observed that while the cathodic peak currents and the maxima of the color intensity derivative vary linearly with the scan rate, for the anodic process the variation is linear with the square root of the scan rate. This is interpreted for the cathodic process, the rate control of these electrochemical processes is given by the kinetics of the process, while for the anodic process it appears to be a transport control. To understand this point, it must be taken into account that the transport control can be due to the transport of electroactive species to or from the solution, but also the transport of electrons in the conducting polymer. Once reduced, the polymer loses its planarity by the reduction of some double bonds and this means that it can also lose part of its conductive properties by losing part of the conjugated double bond structure[13,15]. In other words, this transport control may also indicate that the polymer is less conductive in its reduced form.

2.5. pH Dependence of Voltammetric Peaks

Finally, we study the dependence on the pH of voltametric peaks in order to through light into the mechanism by which electrochemical reactions take place. Figure 10 shows the voltammograms obtained at pH=1.02, pH=3.12 and pH=5.72 at a rate of 10 mV s^{-1} and in a 0.5M KNO_3 solution. First of all, it should be noted that the potential window is different in the three cases. This is because the electrochemical response of this system is highly dependent on the pH of the solution. It is already known that the reduction of the monomer requires the protonation of different centers in the ring and terminal amino groups[43].

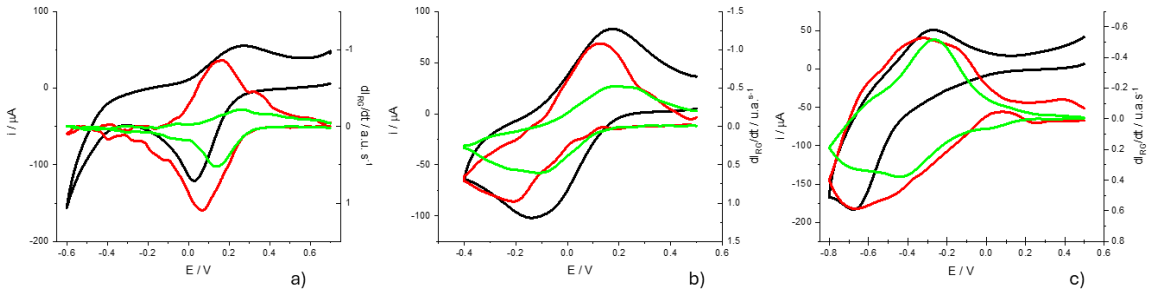

Figure 10. Cyclic voltammograms with color changes of PMB films in 0.5 M KNO_3 solutions at different pH. a) pH 1.02, b) pH= 3.12, c) pH= 5.72. Scan rate was always 10 mV s^{-1} . Black line corresponds to the current curve, Red and Green lines to the dI_R/dt and dI_G/dt curves, respetively.

Looking at the shape of voltammograms at different pH one can see that the HER takes place together with the electrochemical reduction on the PMB at the pH= 5.72, while is clearly separated at the pH=1.02 voltammogram. While the HER is shifted at room temperature by 59 mV/pH, the redox processes associated with the polymer are shifted more significantly. A first estimate is obtained by plotting the variation of the peak potentials for the current and the color intensity derivatives (Figure 11). The fittings show higher correlation for the peak potentials obtained from the color intensity derivatives than for the overall current. This may be due to the fact that the current is the sum of more than one contribution and the color intensity derivatives are associated with simpler redox processes. On the other hand, it is obtained that the potential of the peak of the dI_G/dt moves about 120 mV /pH while that of the peak of dI_R/dt does so about 160 mV / pH.

Preprints.org (www.preprints.org) | NOT PEER-REVIEWED | Posted: 4 July 2024 doi:10.20944/preprints202407.0460.v1

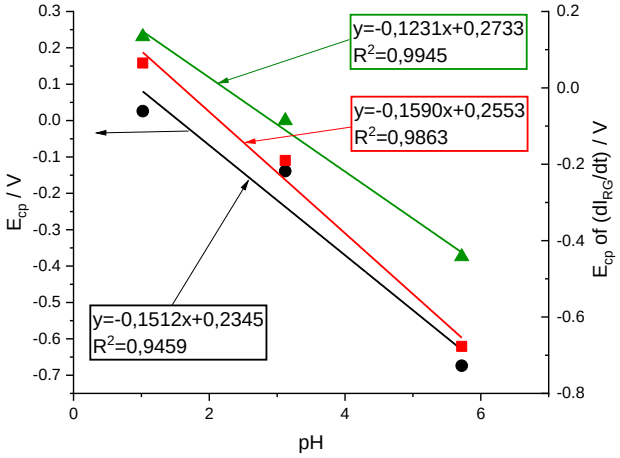

Figure 11. Variación de los potenciales de pico del proceso catódico para la corriente (línea negra) y las derivadas de intensidad de color rojo y verde (líneas roja y verde, respectivamente). Scan rate = 10 mV s^{-1} solution was 0.5 M KNO_3 .

3. Discussion

To further interpret these results, we will consider the proposed reaction mechanisms for monomer reduction. Leventis and Chen proposed that MB gains 3 H^+ during the reduction of the phenothiazine ring involving 2 electrons[43]. Figure 12 shows the proposed reaction at pH<6. In this case, reduction implies a color change from intense blue to the reduced colorless form.

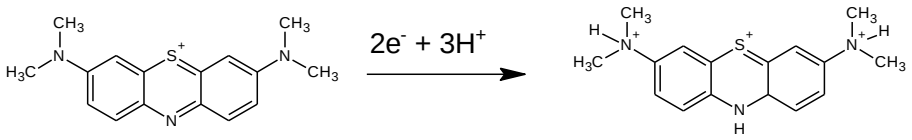

Figure 12. Reduction reaction schema for Methylene Blue reduction if pH<6[43].

If we compare with the case of PMB and according to what we had discussed above, we can assign the process of reduction of the phenothiazine ring to the changes of Red color intensity. If we focus on the Green color changes that we have associated with the electroactive processes of the bridges between monomeric units, we observe a shift of 120 mV/pH, which means that the reduction mechanism involves the insertion of two protons before the first electron transfer[44]. Since there are two amino groups, these two protons can go to the amino groups. After this protonation, there is the electrochemical reduction process associated with the bridges. However, this is not the reaction causing most of the color change of the PMB. The Red color associated reduction reaction which takes place at more negative potentials occurs after and, accordingly with the mechanism proposed for the MB reduction, needs the amino groups to be protonated. However, this reaction only needs one more proton to be fixed on the nitrogen of the phenothiazine ring.

Then a compatible mechanism for the reduction process with those results could be a first step of protonation ($2H^+$) and then a transfer of 2 electrons. This process is associated with Green color changes

$$< Polymer > +2H^+ \rightleftarrows < Polymer, 2H^+(amino) >$$
$$< Polymer, 2H^+(amino) > +2e^- \rightleftarrows < Polymer, 2H^+(amino\ centers\ reduced) >$$

Figure 13. Reduction reaction schema for Methylene Blue reduction if pH<6.

A second step of this mechanism will be the protonation of the nitrogen in the phenothiazine ring and then the electrochemical reduction of the structure which causes the disappearance of the characteristic blue color. Since this second step needs the previous protonation of the amino groups,

 doi:10.20944/preprints202407.0460.v1

apparently 3 H^+ are needed before the first electron transfer. This mechanism also explains a 160 mV/pH dependence of the Red color peak intensity.

As it concerns the oxidation process, it is observed that the electrochromic efficiency values obtained in the cathodic peak zone do not allow such an accurate simulation of the anodic current. This fact together with the fact that the anodic peak intensities vary with the scan rate with a lower slope than the cathodic peak intensities and that the anodic peak appears generally smaller and wider allows us to assume that the oxidation mechanism is different from the reduction mechanism. This will require further investigation.

4. Materials and Methods

All chemical products were commercial. HCl 37%, reagent grade, ACS, ISO (Scharlau); KOH (Merck, for analysis); Methylene Blue (Fluka); KNO3 (Emsure, for analysis); HNO3 60%, extra pure (Scharlau) ; $Na_2C_2O_4$, extra pure (Panreac) ; EtOH absolute, spectroscopy grade (Spectrosol) ; CH_3COOH, synthesis grade (Scharlau). Water was deionized (MilliQ-plus, Millipore, resistivity 18.2 MΩ cm).

For the MB solution, firstly 0.0077 g of MB were weighed, over these 1 mL of absolute ethanol and 0.4 mL of acetic acid were added and this was taken to a 0.01 M solution of $Na_2C_2O_4$ in water. Then, the pH of the solution was adjusted by adding KOH or HCl aqueous solutions previously prepared. Two different solutions were tested: acid solution (pH 1.67) with 0.1 M HCl and basic solution (pH=11.79) with 0.1 M KOH. Deposition was carried out by Cyclic Voltammetry in the potential ranged from -0.4 V to 1.0 V at a scan rate of 20 mV s^{-1} during 100 cycles[45]. The SS316 electrodes were mechanically polished before the deposition to remove any remaining passivate layers or other unwanted substances, then washed with ethanol and deionized water.

The characterization studies were carried out in 0.5 M KNO_3 aqueous solutions where the pH was adjusted by adding 0.1 M KOH or 0.1 M HNO_3 solutions until the desired pH was reached.

pH was measured with a pH Meter, 0.00 – 14.00 pH Measurement Range pH Tester, Digital pH Meter. Characterization studies at three different pH were performed (pH= 1.02, pH=3.12 and pH=5.72). At pH=3.12 the effect of scan rate on the peak currents and peak derivatives of color intensities was made (2 mV s^{-1} to 200 mV s^{-1}) in the potential range [-0.4;0.5] V. At pH =1.02 voltammogram was obtained at 10 mV s^{-1} in the potential range [-0.6;0.7] V and at pH= 5.72 voltammogram was obtained at 10 mV s^{-1} in the potential range [-0.8;0.5] V.

All the electrochemical experiments were carried out in a typical three electrodes cell, where the reference was Ag|AgCl, the auxiliary was a Pt mesh and the working electrode was a 6x1 cm SS316 sheet covered with Teflon tape, leaving an uncovered surface of 1x1 cm at the end of the sheet. The electrochemical cell was an optical quality glass cell of 4cm x2cm. During the characterization experiments a HUE HD Pro Camera, Model: PC0000 (S0011) was attached to the cell, which allows recording video at 30 frames/s with 8 bit depth and 1280x720 pixels resolution. The Potentiostat-Galvanostat μStat400 was used for the electrogeneration studies and the AUTOLAB PGSTAT 302 for the characterization experiments.

Characterization experiments were conducted in a home-made white box illuminated by a LED lamp (6500 K, 10 W).**Figure 14** shows the experimental setup of this spectroelectrochemical cell.

 doi:10.20944/preprints202407.0460.v1

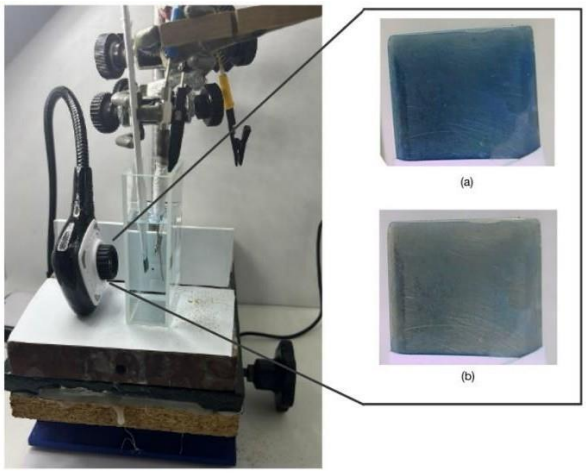

Figure 14. Experimental setup for video acquisition during electrochemical experiments.

Acquired video was analyzed with the help of home-made software for this purpose. Each video was separated into individual images from which the color evolution of the region corresponding to the electrode surface was analyzed. For a better understanding of the results, the mean color intensities for the three channels ($\bar{I}_C$) of a digital image (Red, Green and Blue) were obtained for each frame from Equation (4) thus obtaining the temporal evolution of these parameters.

$$\bar{I}_C = \sum_{j=1}^{n_p} \frac{I_C(j)}{n_p} \quad (4)$$

where n_p is the number of pixels of the analyzed region of the digital image.

The analysis of the digital images is carried out with software programmed at the Electrochemistry Laboratory of the University of Valencia.

5. Conclusions

Methylene Blue can be polymerized on the surface of stainless steel 316 electrodes if prepared in a medium that protects the monomer from possible degradation due to the presence of reactive oxygen species at potentials where the radical cation monomer formation takes place. This medium must be sufficiently basic, and the addition of oxalate anions allows the stabilization of the monomer.

The polymer shows electrochromic activity that is highly dependent on pH. Video electrochemical analysis (DVEC) shows that the electroactive process associated with the phenothiazine ring is associated with Red color intensity changes, while the electroactive processes associated with the new bridges between monomeric units are associated with Green color intensity changes.

The shift of peak potentials with pH allows postulating a possible mechanism for the reduction process while two protons enter the polymer before the first electron transfer associated with the Green color intensity processes and a third proton should enter the film before the reduction process of the phenothiazine ring associated with the red color changes.

Finally, and as a methodological conclusion, it is stated that the use of video electrochemistry together with electrochemical techniques provides valuable information on mechanistic aspects of complex electrochromic processes.

Author Contributions: Conceptualization, JJGJ, JA and FV; methodology, JJGJ, JA, ZV and FV.; software, JJGJ and JA.; validation, JJGA, JA, FV and ZV; formal analysis, JJGJ, JA and ZV; investigation, JJGJ, JA, FV and ZV.; resources, JJGJ, JA and FV.; data curation, JJGJ, JA and ZV; writing—original draft preparation, JA and ZV; writing—review and editing, JJGJ, JA, ZV and FV; visualization, JJGJ, JA and ZV; supervision, JJGJ, FV and JA; project administration, JJGJ, FV and JA; funding acquisition, JJGJ, JA and FV. All authors have read and agreed to the published version of the manuscript.

Funding: This research was funded by Spanish E3TECH-PLUS Research Network, grant number RED2022-134552-T, MICINN/AEI and The APC was waived by invitation.

Institutional Review Board Statement: Not applicable.

Informed Consent Statement: Not applicable.

Data Availability Statement: Data available under demand.

Acknowledgments: The authors acknowledge funding from University of Valencia.

Conflicts of Interest: The authors declare no conflicts of interest.

References

1. Le, T.-H.; Kim, Y.; Yoon, H. Electrical and Electrochemical Properties of Conducting Polymers. *Polymers* **2017**, *9*, 150, doi:10.3390/polym9040150.
2. Shirakawa, H.; Louis, E.J.; MacDiarmid, A.G.; Chiang, C.K.; Heeger, A.J. Synthesis of Electrically Conducting Organic Polymers: Halogen Derivatives of Polyacetylene, (CH). *J Chem Soc Chem Commun* **1977**, 578–580, doi:10.1039/C39770000578.
3. Jones, M.B.; Kovacic, P. 27 - Polyphenylenes. In *Comprehensive Polymer Science and Supplements*; Allen, G., Bevington, J.C., Eds.; Pergamon: Amsterdam, 1989; pp. 465–472 ISBN 978-0-08-096701-1.
4. Goyal, M.; Singh, K.; Bhatnagar, N. Conductive Polymers: A Multipurpose Material for Protecting Coating. *Prog. Org. Coat.* **2024**, *187*, 108083, doi:10.1016/j.porgcoat.2023.108083.
5. Amemiya, T.; Hashimoto, K.; Fujishima, A.; Itoh, K. Analyses of Spectroelectrochemical Behavior of Polypyrrole Films Using the Nernst Equation "Monomer Unit Model" and Polaron/Bipolaron Model. *J. Electrochem. Soc.* **1991**, *138*, 2845–2850, doi:10.1149/1.2085327.
6. Gabrielli, C.; Garcia-Jareno, J.J.; Keddam, M.; Perrot, H.; Vicente, F. Ac-Electrogravimetry Study of Electroactive Thin Films. II. Application to Polypyrrole. *J. Phys. Chem. B* **2002**, *106*, 3192–3201, doi:10.1021/jp013925p.
7. Dian, G.; Barbey, G.; Decroix, B. Electrochemical Synthesis of Polythiophenes and Polyselenophenes. *Synth. Met.* **1986**, *13*, 281–289, doi:10.1016/0379-6779(86)90189-X.
8. Akhtar, M.; Weakliem, H.A.; Paiste, R.M.; Gaughan, K. POLYANILINE THIN-FILM ELECTROCHROMIC DEVICES. *Synth. Met.* **1988**, *26*, 203–208.
9. Fraoua, K.; Delamar, M.; Andrieux, C.P. Study of pH Effect on the Relaxation Phenomenon of Polyaniline by Electrochemistry and XPS. *J. Electroanal. Chem.* **1996**, *418*, 109–113, doi:10.1016/S0022-0728(96)04771-7.
10. Heinze, J.; Frontana-Uribe, B.A.; Ludwigs, S. Electrochemistry of Conducting Polymers—Persistent Models and New Concepts. *Chem. Rev.* **2010**, *110*, 4724–4771, doi:10.1021/cr900226k.
11. Naveen, M.H.; Gurudatt, N.G.; Shim, Y.-B. Applications of Conducting Polymer Composites to Electrochemical Sensors: A Review. *Appl. Mater. Today* **2017**, *9*, 419–433, doi:10.1016/j.apmt.2017.09.001.
12. Introduction of Conducting Polymers. In *Conducting Polymers with Micro or Nanometer Structure*; Wan, M., Ed.; Springer Berlin Heidelberg: Berlin, Heidelberg, 2008; pp. 1–15 ISBN 978-3-540-69323-9.
13. Agrisuelas, J.; Giménez-Romero, D.; García-Jareño, J.J.; Vicente, F. Vis/NIR Spectroelectrochemical Analysis of Poly-(Azure A) on ITO Electrode. *Electrochem. Commun.* **2006**, *8*, 549–553, doi:10.1016/j.elecom.2006.01.022.
14. Karyakin, A.A.; Bobrova, O.A.; Karyakina, E.E. Electroreduction of NAD(+) to Enzymatically Active NADH at Poly(Neutral Red) Modified Electrodes. *J. Electroanal. Chem.* **1995**, *399*, 179–184, doi:10.1016/0022-0728(95)04300-4.
15. Agrisuelas, J.; Gabrielli, C.; García-Jareño, J.J.; Gimenez-Romero, D.; Perrot, H.; Vicente, F. Spectroelectrochemical Identification of the Active Sites for Protons and Anions Insertions into Poly-(Azure A) Thin Polymer Films. *J. Phys. Chem. C* **2007**, *111*, 14230–14237, doi:10.1021/jp0741197.
16. Lim, D.-J. Methylene Blue-Based Nano and Microparticles: Fabrication and Applications in Photodynamic Therapy. *Polymers* **2021**, *13*, 3955, doi:10.3390/polym13223955.
17. Bojadzic, D.; Alcazar, O.; Buchwald, P. Methylene Blue Inhibits the SARS-CoV-2 Spike–ACE2 Protein-Protein Interaction–a Mechanism That Can Contribute to Its Antiviral Activity Against COVID-19. *Front. Pharmacol.* **2021**, *11*, doi:10.3389/fphar.2020.600372.
18. Agostinis, P.; Berg, K.; Cengel, K.A.; Foster, T.H.; Girotti, A.W.; Gollnick, S.O.; Hahn, S.M.; Hamblin, M.R.; Juzeniene, A.; Kessel, D.; et al. Photodynamic Therapy of Cancer: An Update. *CA. Cancer J. Clin.* **2011**, *61*, 250–281, doi:10.3322/caac.20114.
19. Acedo, P.; Stockert, J.C.; Cañete, M.; Villanueva, A. Two Combined Photosensitizers: A Goal for More Effective Photodynamic Therapy of Cancer. *Cell Death Dis.* **2014**, *5*, e1122–e1122, doi:10.1038/cddis.2014.77.
20. de Freitas, L.; Lorenzón, E.; Santos-Filho, N.; Zago, L.; Uliana, M.; Oliveira, K.; Cilli, E.; Fontana, C. Antimicrobial Photodynamic Therapy Enhanced by the Peptide Aurein 1.2. *Sci. Rep.* **2018**, *8*, doi:10.1038/s41598-018-22687-x.

21. Liu, Y.; Zhao, Y.; Wang, J. Fenton/Fenton-like Processes with in-Situ Production of Hydrogen Peroxide/Hydroxyl Radical for Degradation of Emerging Contaminants: Advances and Prospects. *J. Hazard. Mater.* **2021**, *404*, 124191, doi:10.1016/j.jhazmat.2020.124191.
22. Brillas, E. Fenton, Photo-Fenton, Electro-Fenton, and Their Combined Treatments for the Removal of Insecticides from Waters and Soils. A Review. *Sep. Purif. Technol.* **2022**, *284*, 120290, doi:10.1016/j.seppur.2021.120290.
23. Sahoo, M. Degradation and Mineralization of Organic Contaminants by Fenton and Photo-Fenton Processes: Review of Mechanisms and Effects of Organic and Inorganic Additives. *Res. J. Chem. Environ.* **2011**, *15*, 96–112.
24. Satoh, A.Y.; Trosko, J.E.; Masten, S.J. Methylene Blue Dye Test for Rapid Qualitative Detection of Hydroxyl Radicals Formed in a Fenton's Reaction Aqueous Solution. *Environ. Sci. Technol.* **2007**, *41*, 2881–2887, doi:10.1021/es0617800.
25. Wang, S.; Zhang, Y. Degradation of Methylene Blue by an E-Fenton Process Coupled with Peroxymonosulfate via Free Radical and Non-Radical Oxidation Pathways. *New J. Chem.* **2023**, *47*, 3616–3627, doi:10.1039/D2NJ05504J.
26. Blubaugh, E.A.; Yacynych, A.M.; Heineman, W.R. Thin-Layer Spectroelectrochemistry for Monitoring Kinetics of Electrogenerated Species. *Anal. Chem.* **1979**, *51*, 561–565, doi:10.1021/ac50040a026.
27. Garoz-Ruiz, J.; Perales-Rondon, J.V.; Heras, A.; Colina, A. Spectroelectrochemical Sensing: Current Trends and Challenges. *Electroanalysis* **2019**, *31*, 1254–1278, doi:10.1002/elan.201900075.
28. Agrisuelas, J.; García-Jareño, J.J.; Perianes, E.; Vicente, F. Use of RGB Digital Video Analysis to Study Electrochemical Processes Involving Color Changes. *Electrochem. Commun.* **2017**, *78*, 38–42, doi:10.1016/j.elecom.2017.04.001.
29. Agrisuelas, J.; García-Jareño, J.J.; Vicente, F. Quantification of Electrochromic Kinetics by Analysis of RGB Digital Video Images. *Electrochem. Commun.* **2018**, *93*, 86–90, doi:10.1016/j.elecom.2018.06.011.
30. Guillén, E.; Agrisuelas, J.; García-Jareño, J.J.; Vicente, F. Electrochromic Performances of Poly(Azure A) Films from Digital Video-Electrochemistry (DVEC). *J. Electrochem. Soc.* **2020**, *167*, 106514, doi:10.1149/1945-7111/ab9e3b.
31. Agrisuelas, J.; García-Jareño, J.J.; Guillén, E.; Vicente, F. Kinetics of Surface Chemical Reactions from a Digital Video. *J. Phys. Chem. C* **2020**, *124*, 2050–2059, doi:10.1021/acs.jpcc.9b10689.
32. Agrisuelas, J.; García-Jareño, J.J.; Vicente, F. A Statistical Interpretation of the Voltammetry of Adsorbed Substances under the Perspective View of the Digital Video Electrochemistry. *Microchem. J.* **2022**, *181*, 107844, doi:10.1016/j.microc.2022.107844.
33. Fenelon, A.M.; Breslin, C.B. An Investigation into the Degradation of Polyaniline Films Grown on Iron from Oxalic Acid. *Synth. Met.* **2004**, *144*, 125–131, doi:10.1016/j.synthmet.2004.02.014.
34. Agrisuelas, J.; Ferrus, D.; Gabrielli, C.; García-Jareño, J.J.; Perrot, H.; Sel, O.; Vicente, F. Poly(Neutral Red) on Passivated Nickel Films. New Insights Through EQCM Measurements. *Russ. J. Electrochem.* **2016**, *52*, 1137–1149, doi:10.1134/S1023193516120028.
35. Roullier, L.; Laviron, E. Effect of Uncompensated Ohmic Drop in Surface Linear Potential Sweep Voltammetry: Application to the Determination of Surface Rate Constants. *J. Electroanal. Chem. Interfacial Electrochem.* **1983**, *157*, 193–203, doi:10.1016/S0022-0728(83)80350-7.
36. García-Jareño, J.J.; Navarro-Laboulais, J.; Vicente, F. A Numerical Approach to the Voltammograms of the Reduction of Prussian Blue Films on ITO Electrodes. *Electrochimica Acta* **1997**, *42*, 1473–1480, doi:10.1016/S0013-4686(96)00302-7.
37. Agrisuelas, J.; García-Jareño, J.J.; Guillén, E.; Vicente, F. RGB Video Electrochemistry of Copper Electrodeposition/Electrodissolution in Acid Media on a Ternary Graphite:Copper:Polypropylene Composite Electrode. *Electrochimica Acta* **2019**, *305*, 72–80, doi:10.1016/j.electacta.2019.03.016.
38. Guillén, E.; Ferrer-Roselló, M.; Agrisuelas, J.; García-Jareño, J.J.; Vicente, F. Digital Video-Electrochemistry (DVEC) to Assess Electrochromic Materials in the Frequency Domain: RGB Colorimetry Impedance Spectroscopy. *Electrochimica Acta* **2021**, *366*, 137340, doi:10.1016/j.electacta.2020.137340.
39. Laviron, E. Surface Linear Potential Sweep Voltammetry: Equation of the Peaks for a Reversible Reaction When Interactions between the Adsorbed Molecules Are Taken into Account. *J. Electroanal. Chem. Interfacial Electrochem.* **1974**, *52*, 395–402, doi:10.1016/S0022-0728(74)80449-3.
40. Peerce, P.J.; Bard, A.J. Polymer Films on Electrodes: Part III. Digital Simulation Model for Cyclic Voltammetry of Electroactive Polymer Film and Electrochemistry of Poly(Vinylferrocene) on Platinum. *J. Electroanal. Chem. Interfacial Electrochem.* **1980**, *114*, 89–115, doi:10.1016/S0022-0728(80)80438-4.
41. García-Jareño, J.J.; Agrisuelas, J.; Vicente, F. Overview and Recent Advances in Hyphenated Electrochemical Techniques for the Characterization of Electroactive Materials. *Materials* **2023**, *16*, 4226, doi:10.3390/ma16124226.
42. Agrisuelas, J.; García-Jareño, J.J.; Vicente, F. Spatiotemporal Colorimetry to Reveal Electrochemical Kinetics of Poly(o-Toluidine) Films along ITO Surface. *Electrochimica Acta* **2018**, *269*, 350–358, doi:10.1016/j.electacta.2018.02.157.

 doi:10.20944/preprints202407.0460.v1

43. Leventis, N.; Chen, M. Electrochemically Assisted Sol−Gel Process for the Synthesis of Polysiloxane Films Incorporating Phenothiazine Dyes Analogous to Methylene Blue. Structure and Ion-Transport Properties of the Films via Spectroscopic and Electrochemical Characterization. *Chem. Mater.* **1997**, *9*, 2621–2631, doi:10.1021/cm970261g.
44. Bard, A.J.; Faulkner, L.R. *Electrochemical Methods: Fundamentals and Applications*; 2nd Edition.; Wiley: New York, 2000; ISBN 978-0-471-04372-0.
45. Karyakin, A.A.; Strakhova, A.K.; Karyakina, E.E.; Varfolomeyev, S.D.; Yatsimirsky, A.K. The Electrochemical Polymerization of Methylene Blue and Bioelectrochemical Activity of the Resulting Film. *Bioelectrochem. Bioenerg.* **1993**, *32*, 35–43, doi:10.1016/0302-4598(93)80018-P.